Available at www.sciencedirect.com

ScienceDirect

journal homepage: www.elsevier.com/locate/he

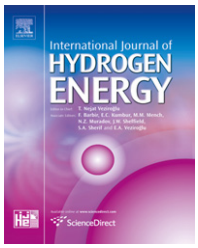

Complexation in the Cu(II)–LiCl–H_2O system at temperatures to 423 K by UV-Visible spectroscopy

Liliana Trevani [a], *Jana Ehlerova* [b], *Josef Sedlbauer* [b], *Peter R. Tremaine* [c,*]

[a] *Faculty of Science, University of Ontario Institute of Technology, Oshawa, Canada L1H 7K4*
[b] *Department of Chemistry, Technical University of Liberec, 46117 Liberec, Czech Republic*
[c] *Department of Chemistry, University of Guelph, Guelph, Ontario, Canada N1G 2W1*

ARTICLE INFO

Article history:
Received 30 June 2009
Received in revised form
8 October 2009
Accepted 14 October 2009
Available online 13 November 2009

Keywords:
Hydrogen
Thermochemical cycles
Copper-chloride cycle
Copper-chloride complexation reactions
Hydrothermal systems
High-temperature spectroscopy
UV-visible spectroscopy

ABSTRACT

Thermodynamic data for the solubility and formation of copper(I)and copper(II) species are required to model innovative designs of the electrolysis cells used in the thermochemical copper-chloride hydrogen production process. Cumulative formation constants of Cu^{2+}(aq) complexes with Cl^-(aq) were determined by Principal Component Analysis of UV-spectra, obtained over a very wide range of solution compositions and temperature, coupled with an appropriate model for activity coefficients of the solution species. Shortcomings in the existing database and future work to extend these studies to higher temperatures and much higher copper concentrations are discussed.

1. Introduction

The Super-Critical-Water-Cooled Reactor (SCWR) is a concept for a novel, extremely energy-efficient advanced nuclear reactor that has been chosen by Canada as its major R&D contribution to meet the targets of the Generation IV International Forum treaty. A requirement of all the SCWR concept designs is an ability to co-generate hydrogen from high-temperature steam at temperatures below 823 K. The reactor would be separated from the hydrogen production plant, but coupled through an intermediate heat exchanger that supplies heat to the thermochemical cycle.

Over 200 processes for thermal hydrogen production have been evaluated by the US Department of Energy and three have been selected for use at temperatures below 823 K [1]. As yet, only one of these, the copper-chloride cycle, has been shown to have promise as a practical process. The laboratory-scale copper chloride process involves an electrochemical step at temperatures up to 348 K, with chloride concentrations up to ~6 mol kg^{-1}. The Canadian research program is investigating novel electrochemical processes, higher acid concentrations, and the use of temperatures up to 423 K and pressures of 15 MPa, to achieve efficiencies in the electrolysis reactions and the compression of produced hydrogen gas [2,3]. Copper (I) and copper (II) chloride solubilities and data for complex formation are required to model speciation in the aqueous phase and copper transport mechanisms under these conditions [3].

* *Corresponding author*. Tel.: +1 519 824 4120(56076); fax: +1 519 766 1499.
E-mail address: tremaine@uoguelph.ca (P.R. Tremaine).
0360-3199/$ – see front matter
doi:10.1016/j.ijhydene.2009.10.046

Fritz and Königsberger [4] have compiled solubility data for cuprous and cupric chloride, CuCl and $CuCl_2$, in several chloride media including concentrated hydrochloric acid solutions. Unfortunately, there is only one set of data in this compilation that reaches 373 K, and the uncertainty is larger than that for data at lower temperatures. Most of the solubility studies at high-temperature were intended to understand the transport and deposition of copper in ore-forming systems or concentrated brines [5–10]. As a consequence, hydrochloric acid is only present at very low concentrations to avoid the hydrolysis of copper and the formation of hydroxyl-copper species. Cumulative formation constants for chloride with copper (I) and copper (II) have been reported by Liu et al. [9,10] and Brugger et al. [11].

In the case of $CuCl_2$, extensive work has been done in the field of hydrometallurgy, mainly in concentrated $CuCl_2$–NaCl solutions at moderate temperatures [12–14]. Much less has been done on the electrodeposition of copper from $CuCl_2$–HCl solutions, due to the difficulties associated with the use of concentrated HCl solutions [15]. The complexation of copper(II) with chloride was studied by Brugger et al. [11] in LiCl solutions up to 363 K and, according to the authors, there is evidence for the formation of up to four or even five copper complexes. There are no other accurate data for polynuclear copper complexes above 298 K.

In the first phase of this study, we have used the high-temperature UV-visible flow system developed by Trevani et al. [16] to measure the spectra of Cu(II)–LiCl–H_2O solutions at 373 K and 423 K, at a pressure of 9 MPa. The spectra were obtained for solutions with constant initial loading of copper and at different concentrations of LiCl, from 0 mol kg^{-1} to 15 mol kg^{-1}. A small excess of hydrochloric acid was used to prevent the precipitation of hydroxides. Under these conditions, complexation is expected to take place by successive displacement of water molecules according to the reaction:

$$\left[Cu(H_2O)_6\right]^{2+} + nCl^-(aq) \rightleftarrows \left[CuCl_n(H_2O)_{6-n}\right]^{2-n} + nH_2O; \quad n = 1-4 \tag{1}$$

These measurements are part of a broader project involving the study of complexation reactions in concentrated HCl solutions up to 6 mol kg^{-1}, and Cu(II) concentrations up to the solubility limit. The experimental information will be used to model the solubility of copper in the electrochemical step of the copper thermochemical cycle. LiCl was chosen as the source of chloride because at our experimental conditions this electrolyte is more benign compared to other salts, and is consistent with other experimental studies in the literature [11,12]. This point is important because the high number of absorbing species in the solution requires the use of factor analysis methods in the data treatment and a very wide range of concentrations [17].

2. Experimental

2.1. Chemicals

All chemical materials were used without further purification. The list of chemicals includes: lithium chloride, LiCl (Sigma–Aldrich, 99+%, A.C.S. reagent); sodium hydroxide, NaOH (50% w/w solution, Fisher ACS certified); hydrochloric acid, HCl (ACS reagent-grade); copper(II) chloride dihydrate, $CuCl_2.2H_2O$ (Sigma–Aldrich, 99.99+%); silver nitrate, $AgNO_3$ (Fisher ACS certified); potassium chromate, K_2CrO_4 (Fisher ACS certified); potassium thiocyanate, KSCN (BDH, 98%, analytical reagent); sodium thiosulphate pentahydrate, $Na_2S_2O_3.5H_2O$ (Fisher ACS certified); sodium carbonate, Na_2CO_3 (Fisher-Scientific); potassium iodate, KIO_3 (Caledon, 99.4%); potassium iodide, KI (Fisher, Reagent A.C.S.); starch (Fisher-Scientific, starch solution stabilized); sodium chloride, NaCl (Sigma Ultra, 99.5%). Solutions were prepared by mass using nanopure water (resistivity > 18 MΩ cm).

The concentrations of the $CuCl_2$, LiCl, and HCl stock solutions used to prepare the final $CuCl_2$–HCl–LiCl solutions were determined by titration against standard $Na_2S_2O_3$, $AgNO_3$, and NaOH solutions, respectively [18,19]. All titrations were done by mass. The molality of the $Na_2S_2O_3$ solution was determined by titration against a primary standard KIO_3 solution using the starch indicator. $AgNO_3$ solution was standardized against a primary standard NaCl solution using a K_2CrO_4 indicator. The NaCl salt was dried for at least 48 h at 393 K before preparing the solution. The molality of the HCl stock solution was determined by titration against a secondary standard NaOH(aq) solution that was previously standardized by titration against a primary standard, potassium hydrogen phthalate (Fisher-Scientific), which was dried for at least 48 h at 393 K before preparing the solution. The acid-base titrations were done by mass using a Metrohm794 basic Titrino titrator.

LiCl–HCl solutions with chloride concentrations from ~0 to 15 mol kg^{-1} were prepared by mass from standard LiCl and HCl solutions and with deionized nanopure water. Each solution was divided in two parts. $CuCl_2$–HCl stock solution was added to one of the fractions to obtain a total copper concentration of $\sim 10^{-4}$ mol kg^{-1} while the other without copper was used to run the baseline experiments.

2.2. Experimental measurements

UV-visible spectra were measured in a high-temperature, high-pressure titanium cell with sapphire windows (1.72 cm optical path length; 0.34 cm^3 volume) described by Trevani et al. [16]. The sample injection system was modified to allow the automatic injection of the solutions (see Fig. 1). The current design is based on a system developed by Mendez de Leo and Wood [20] for high-temperature and high-pressure conductance measurements. In our system, the only materials in contact with the solutions were PEEK (polyaryletheretherketone), PTFE (polytetrafluoroethylene), titanium (Grade 2), sapphire, and Pyrex glass. In this system, the low-pressure peristaltic pump was used to fill the sample loop through a low-pressure 12 port valve connected by PTFE tubing to 12 different glass bottles containing the solutions. A high-performance liquid chromatography pump (HPLC Gilson 305) was used to inject the solutions contained in the sample injection loop into the cell (low rate ~0.5 $cm^3\,min^{-1}$). A high-pressure 6 port valve allowed the operator to select deionized water or the solution in the injection loop (copper chloride or baseline solution). In our design and because of the temperature range, the solutions were not pressurized before injecting them into the system. The second high-pressure 6 port valve

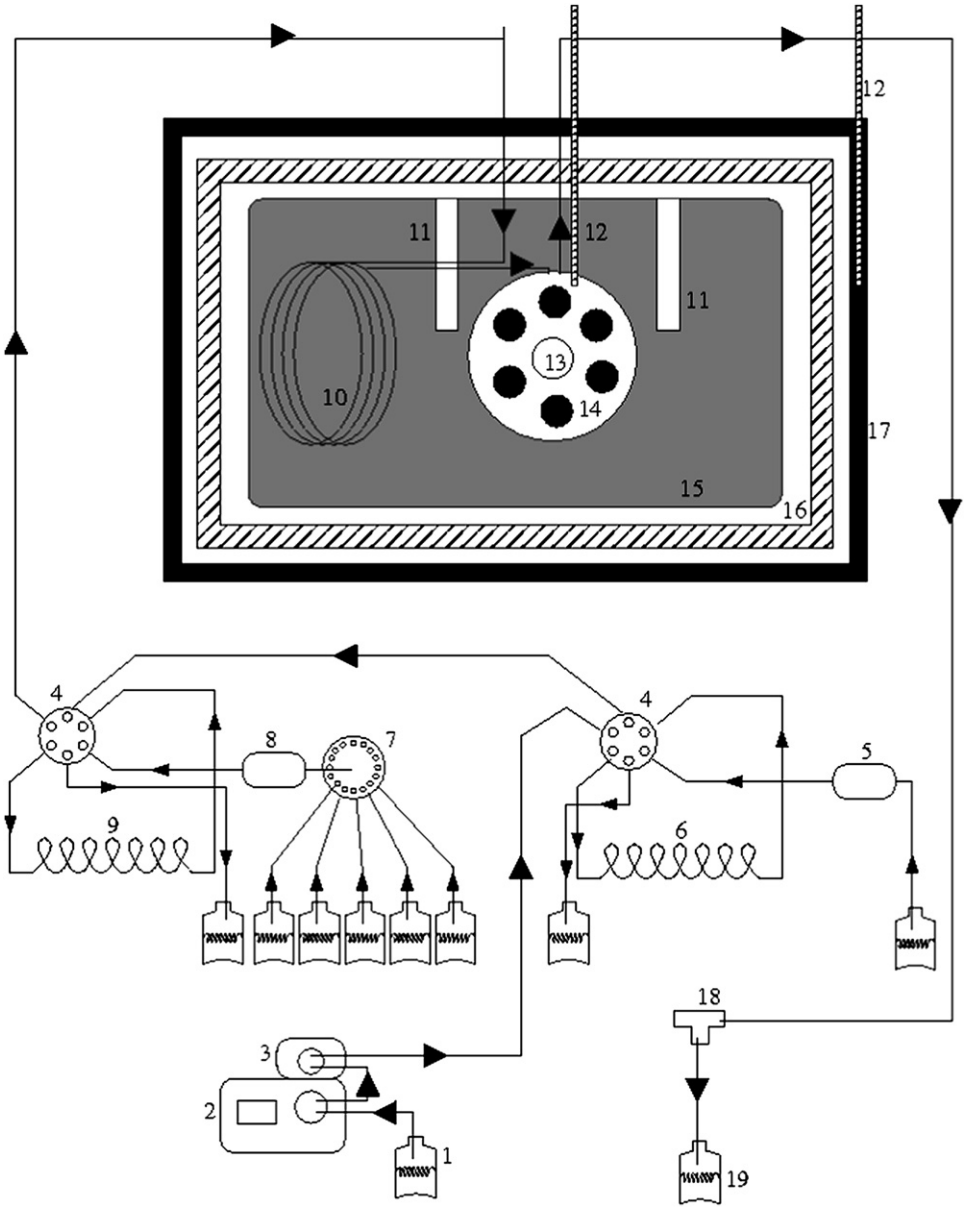

Fig. 1 – UV-visible flow cell and high-pressure injection system: (1) deionized water, (2) HPLC pump, (3) pressure transducer, (4) HP 6 port valves, (5) auxiliary peristaltic pump, (6) HCl cleaning solution injection loop, (7) 12 port low-pressure valve, (8) peristaltic pump, (9) PEEK injection loop, (10) titanium pre-heater, (11) heaters, (12) thermocouple, (13) sapphire windows, (14) titanium cell, (15) oven, (16) thermal insulation, (17) water cooling box, (18) rupture disc, and (19) waste bottle.

was used to switch between the baseline/copper solutions and a dilute acid solution used to periodically clean the system. A back-pressure regulator was used to keep the pressure of the system at 9 MPa.

A Varian Cary 50 spectrophotometer (190–1100 nm) interfaced to a computer with Cary Win UV Scan Application software was used to record the absorption spectra at two different temperatures 373 K and 423 K. All spectra (baseline and copper solutions) were collected at 1 nm wavelength intervals from 200 nm to 1100 nm at a scan rate 600 nm min^{-1}. Five consecutive scans in a ten-minute period were obtained for each sample and the spectra were averaged to minimize noise. At a flow rate of 0.5 cm^3 min^{-1} it took approximately 4 min to reach the target temperature (±0.1 K). For the most concentrated LiCl solutions, about 8 min was required, in the worst case, to reach a constant spectrum because of the density and viscosity differences between water and the sample solutions.

2.3. *Analysis of the spectroscopic data*

According to the Beer's law, the absorbance of a solution containing multiple absorbing species can be written as

$$A(\lambda) = \sum \varepsilon_i(\lambda) b C_i \quad (2)$$

where $\varepsilon_i(\lambda)$ and C_i are the molar absorptivity and molar concentration of species *I*, respectively, and *b* is the optical

path length. For convenience, we have chosen to adopt a different concentration scale using units of mol per kg of solvent, rather than the usual molarity scale. To account for this transformation, a correction factor, $f(\rho)$, had to be introduced in Eq. (2).

$$A(\lambda)/f(\rho_i) = \sum \varepsilon_i(\lambda) b m_i \quad (3)$$

with

$$f(\rho_i) = 1000\rho_{LiCl}/(1000 + m_{LiCl}M_{LiCl}) \quad (4)$$

where ρ_{LiCl} (kg dm^{-3}) is the density of LiCl solution at the same temperature; $M_{LiCl} = 44.394$ g mol^{-1} is the molar mass of LiCl; and m_{LiCl} (mol kg^{-1}) is the molality of LiCl in our solutions. The density of the LiCl solutions was calculated from the correlation by Abdulagatov and Azizov [21]. The effect of solutes other than LiCl on the density of the solutions is neglected in Eq. (4), which is an acceptable approximation for our LiCl-dominated systems.

3. Results and discussion

The baseline-corrected absorbance data shown in Fig. 2 were used for qualitative as well as quantitative analyses of complex formation in the copper-chloride systems. In addition to the complexation reactions (1), other reactions can take place, such as the formation of neutral ion pairs, HCl^0,aq and $LiCl^0$,aq, at the concentration and temperature ranges covered in this study. The formation of polynuclear copper complexes was not considered in the data treatment since the concentration of copper is typically several orders of magnitude lower than that of the chloride.

3.1. Qualitative analysis

The first estimate of the number of absorbing aqueous species required to describe the experimental absorbance data was carried out using principal component analysis, ''PCA'' [17]. At both experimental temperatures, PCA suggested that 5 factors are the minimum number required to achieve a description that is comparable with our experimental uncertainty. As a result, we chose to include the formation of 4 mononuclear complexes up to $[CuCl_4]^{2-}$, in addition to free copper, $[Cu(H_2O)_6]^{2+}$. A solution of Beer's law, Eq. (3), was then obtained using the ''model-free'' approach described e.g. by Brugger et al. [11] with the constraints of positive molar absorptivity coefficients and concentrations, unimodality of the calculated concentration profiles of absorbing species, and fixed mass balance for copper-containing solutes. All calculations were performed with the software package BeerOz [22]. The results of this ''model-free'' regression can be used mainly for preliminary estimation of the relative abundance of absorbing species and for confirmation of the proposed number of factors contributing to absorption. At both experimental temperatures (373 K and 423 K) the distribution of species obtained from the ''model-free'' fit is consistent with our assumption of 5 absorbing factors, with non-negligible concentrations of all copper complexes.

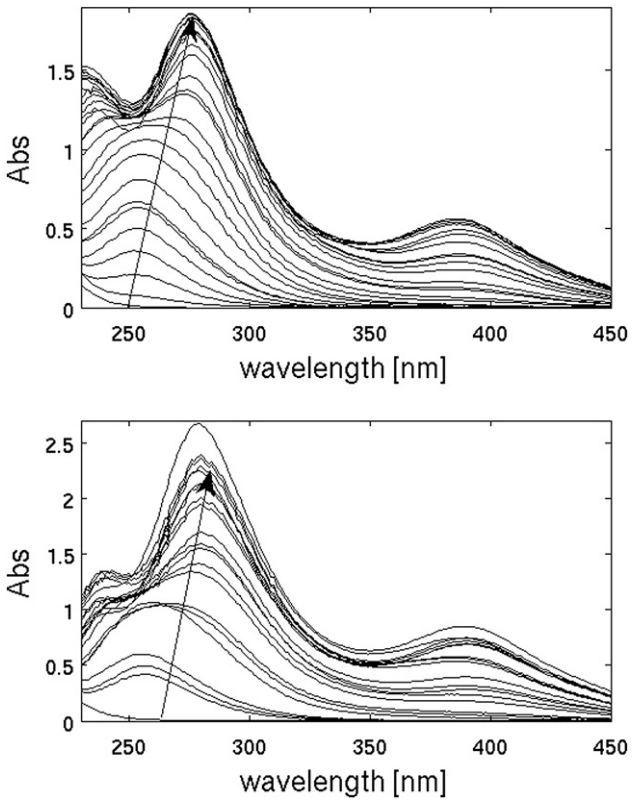

Fig. 2 – Baseline-corrected absorbance data for the copper-chloride system at 373 K (top) and 423 K (bottom). Arrows indicate increasing chloride concentrations.

3.2. Thermodynamic model

In addition to the constraints applied in the ''model-free'' regression to Beer's law, the concentrations of species present in any solution must obey the mass-action laws for association reactions (LiCl, HCl) and complex formation reactions (Eq.(1)), as well as the mass balance equations for total Cu, Cl and Li. Simultaneous treatment of absorption data with all these equations and with a model for the activity coefficients allowed us to derive concentration profiles of absorbing species and their formation constants. Below, we comment on the required input for the thermodynamic model, which includes association constants of HCl and LiCl and an assumption for activity coefficients of all species, ionic and neutral, in the solutions.

As a strong electrolyte, LiCl undergoes dissociation in aqueous solutions, which is almost complete at temperatures below 473 K and at low and moderate solute concentrations. As the temperatures or concentrations of the salt increase, ionic association becomes non-negligible and should be accounted for when modeling the thermodynamic behaviour of such solutions. We have calculated the association constant of LiCl from the Helgeson-Kirkham-Flowers (''HKF'') equation-of-state [23] using parameters of the HKF equation for the ions from Shock et al. [24,25] and for the $LiCl^0$,aq ion pair from Sverjensky et al. [26]. Activity coefficients for Li^+, Cl^- and $LiCl^0$,aq were obtained by the method described below. We assumed that lithium and chloride ions

do not form any other complexes except the $LiCl^0$,aq ion pair, which is a necessary approximation due to unknown character and thermodynamic properties of such possible multiple ion pairs.

A similar procedure was adopted for calculating the association constant for hydrochloric acid, using parameters of the HKF equation for HCl,aq given by Sverjensky et al. [27]. It should be noted that another set of HKF parameters for HCl^0,aq has been reported by Pokrovskii [28], leading to a much different value of the association constant, for example at ~373 K, log *K* (HCl) = −0.7 from ref. [27] and log *K* (HCl) = −3.8 from ref. [28]. This large difference is attributed to the choice of contradictory low-temperature data used by different authors for parameterization of the HKF model. Sverjensky et al. [27] relied mostly on the association constants retrieved from AgCl solubility measurements in HCl solutions by Ruaya and Seward [29], while Pokrovskii preferred the results obtained from HCl to H_2O liquid–vapour equilibrium measurements [30,31]. Fortunately, this considerable uncertainty in the values used for the association constant of HCl is of only minor significance for the thermodynamic treatment of our solutions since hydrochloric acid is always present in small amounts.

Mean stochiometric activity coefficients for LiCl based on the ion-interaction approach [32] were obtained by Holmes and Mesmer [33] from simultaneous correlation of isopiestic, phase equilibrium, electrochemical and calorimetric data to 523 K and ~6 mol kg^{-1}. If ion pairing is accounted for, these stochiometric activity coefficients need to be converted to the individual activity coefficients of the ions and the ion pair. The method that we chose for this purpose is described in detail e.g. by Pokrovskii and Helgeson [34], therefore only the most salient features are given below. Since LiCl is always a dominant electrolyte in our solutions, we assumed that activity coefficients of all our ionic species are the same as for the Li^+ and Cl^- ions (or differ by a constant in the activity coefficient model, see below). Approximations adopted for activity coefficients of neutral molecules are also discussed in the next paragraphs.

Following Pokrovskii and Helgeson [34], the mean activity coefficient for ions is given by

$$\log\gamma_i = -\frac{A|Z_K Z_A| I^{1/2}}{1 + a^\circ B I^{1/2}} + \Gamma + b_i I + b_{i,sq} I^2 \quad (5)$$

where *A* and *B* represent the Debye-Hückel solvent parameters, a° denotes the distance of closest approach in a given salt, Z_K and Z_A are the charges of the cation and anion, respectively, $\Gamma = -\log(1 + 0.018053 m^*)$ designates the mole fraction to molality conversion, m^* is the sum of molalities of all solute species, $I = 1/2 \Sigma m_i Z_i^2$ is the molal-scale ionic strength, b_i represents the extended term for the electrolyte, which is a function of temperature and pressure, and $b_{i,sq}$ term is a further extension of the model used by Pokrovskii and Helgeson [34] for application at molalities over ~10 mol kg^{-1}. The values adopted for a° are 5 Å for divalent ions and 4 Å for monovalent ions, with the exception of H^+ that was given a value of 9 Å. For neutral ion pair $LiCl^0$,aq the activity coefficient was obtained from

$$\log\gamma_n = \Gamma + b_n I \quad (6)$$

where b_n is usually referred to as the Setchénow coefficient. The relation between the stochiometric and individual ionic activity coefficients is given by

$$\gamma^{st} = (1 - \alpha)\gamma_i \quad (7)$$

where α is the degree of association of the electrolyte, calculated from the mass-action law. The following procedure was used to retrieve the parameters b_i, $b_{i,sq}$ and b_n at each temperature:

1) Ionic strength and the degree of association were calculated first, using initial estimates of the parameters b_i, $b_{i,sq}$ and b_n;
2) Parameters b_i, $b_{i,sq}$ were obtained by regression of Eq. (5) against the stochiometric activity coefficients reported by Holmes and Mesmer [33] to ~10 mol/kg;
3) Parameter b_n was calculated from the mass-action law.

Step (1) was repeated with the new set of parameters b_i, $b_{i,sq}$ and b_n. This iterative process proceeded until the calculated activity coefficient parameters were stable. The values of b_i, $b_{i,sq}$ and b_n obtained in this way are (0.105, 0.00125, 0.322) at 373 K and (0.0994, 0.000803, 0.304) at 423 K.

Activity coefficients for neutral molecules other than $LiCl^0$,aq are unknown. We have assumed $b_n = 0$ in Eq. (6) for HCl^0,aq which is a safe approximation in our very dilute solutions of hydrochloric acid. In case of aqueous $CuCl_2^0$ it was

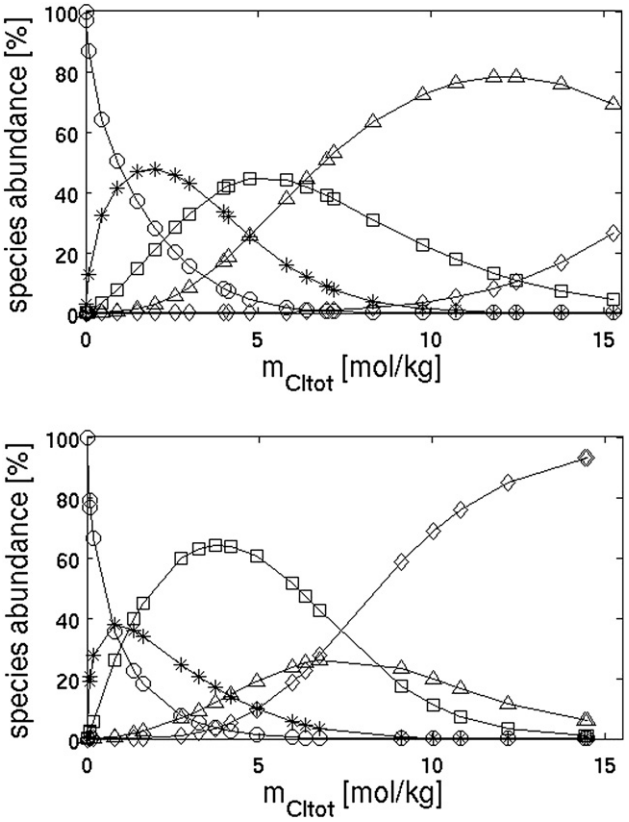

Fig. 3 – Concentration profiles obtained by regression analysis of the experimental baseline-corrected spectra at 373 K (top) and 423 K (bottom). Symbols: (○) $[Cu(H_2O)_6]^{2+}$; (*) $[CuCl]^+$; (◊) $[CuCl_2]^0$; (Δ) $[CuCl_3]^-$; (□) $[CuCl_4]^{2-}$.

Table 1 – Values of log K_n (cumulative formation constants for copper complexes, Eq. (1)) derived from absorbance data.[a]

Temperature/K	Pressure/MPa	log K_1 $[CuCl]^+$	log K_2 $[CuCl_2]^0$	log K_3 $[CuCl_3]^-$	log K_4 $[CuCl_4]^{2-}$	Reference
298	0.1	0.27 (−0.1/+0.1)	−0.63 (−0.1/+0.4)	−2.44 (−0.3/+0.6)	−5.9 (−0.5/+1.0)	[11]
333	0.1	0.53 (−0.1/+0.1)	−0.13 (−0.3/+0.4)	−1.75 (−0.5/+0.4)	−5.1 (−1.0/+1.0)	[11]
363	0.1	0.73 (−0.1/+0.1)	0.36 (−0.3/+0.4)	−1.04 (−0.5/+0.3)	−4.3 (−2.0/+1.0)	[11]
373	9	0.74 (−0.1/+0.2)	0.47 (−0.3/+0.4)	−0.84 (−0.4/+0.2)	−4.6 (−1.0/+1.0)	This work
423	9	1.02 (−0.1/+0.2)	1.44 (−0.3/+0.4)	−0.14 (−0.4/+0.3)	−2.0 (−1.0/+1.5)	This work

a Uncertainty limits are given in parentheses.

observed by Brugger et al. [11] that assigning the Setchénow coefficient in Eq. (6) in a reasonable interval, $0 < b_n < 0.3$, does not affects appreciably the values of the regressed formation constants for copper-chloride complexes but may change considerably the relative distribution of different complexes. Brugger and co-workers adopted $b_n = 0.1$ for the neutral complex, $CuCl_2^0$, which is an "intermediate" value leading to molar absorptivities $\varepsilon_i(\lambda)$ in Eq. (2) that are similar in magnitude for all complexes and to species distribution that does not suppress any of the complexes. We have confirmed these observations during the analysis of our data and applied finally the same approach for the activity coefficient of aqueous $CuCl_2^0$ for the sake of consistency with the previous literature results.

3.3. *Thermodynamics of complex formation*

Regressions with a full thermodynamic model were also performed with the BeerOz software package [22]. All measured spectra were included into evaluation in the wavelength range from 230 nm to 450 nm. Following qualitative analysis by PCA we postulated the model with 5 absorbing species at both temperatures. The calculated concentration profiles (Fig. 3) were physically realistic and relatively insensitive to changes in the database used for the fitting, for example, similar results were obtained after excluding absorbance data at wavelengths below 250 nm and/or excluding the absorbance data at concentrations above 10 mol kg^{-1} or even 6 mol kg^{-1} of Cl_{tot}. The same applies for the numerical stability of the calculated equilibrium constants of complexation reactions (Eq. (1)), although the results at 423 K were more sensitive to changes in the fitting database.

Table 1 summarizes the formation constants obtained in this study at 9 MPa along with the results reported to 363 K at 0.1 MPa by Brugger et al. [11]. The same data are compared in Fig. 4 with the predictions of the HKF equation-of-state based on the parameters for copper complexes from Sverjensky et al. [26]. The lines corresponding to HKF model were calculated along the 9 MPa isobar. The pressure effects under these conditions are small, less than the experimental uncertainties. As a result, the predicted values at 0.1 MPa below 373 K are almost indistinguishable from the 9 MPa line within the scale of Fig. 4 and were thus omitted from the graphics.

Our results at 373 K are in good agreement with the values reported by Brugger et al. [11] at 363 K. The difference is negligible in case of $[CuCl]^+$, small and in trend with the lower temperature results in the case of $[CuCl_2]^0$ and $[CuCl_3]^-$, the only difference outside the trend was found for the $[CuCl_4]^{2-}$ complex. However, uncertainty limits for $[CuCl_4]^{2-}$ formation constant are larger than the observed disagreement between both set of data at these temperatures. Uncertainty limits stated in Table 1 for data taken from Brugger et al. [11]

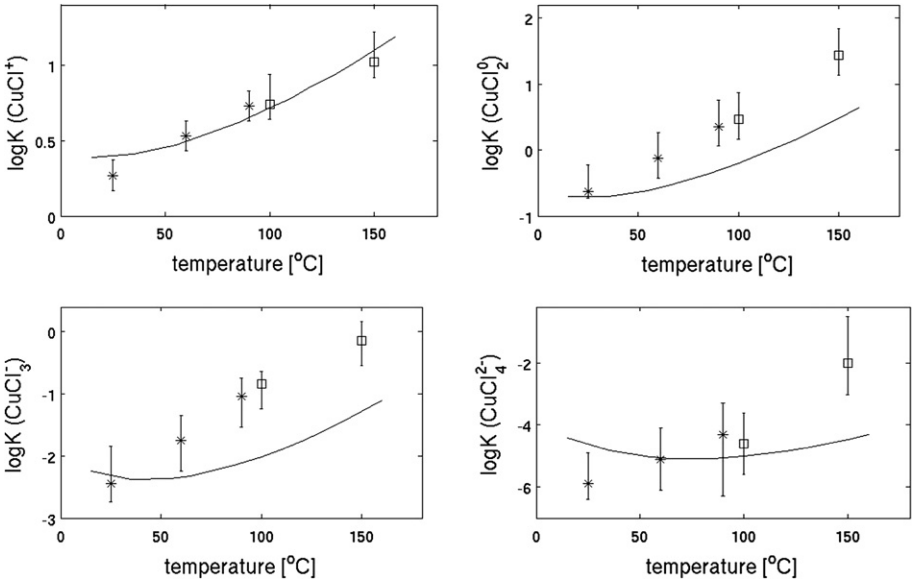

Fig. 4 – log *K* (formation constants for copper complexes, Eq. (1)) as a function of temperature. Symbols: (*) Ref. [11], (ð) this work. Lines: HKF predicted values at 9 MPa (see text for details). Error bars correspond to uncertainty limits as reported in Table 1.

correspond to the minimum and maximum values within the 90% confidence interval of the calculated log *K*, for our results the uncertainties were estimated from the maximum and minimum differences obtained by regressions with database subsets (see above the discussion on numerical stability).

Increasing trends for the dependence of formation constants with temperature are confirmed by our data, although there seem to be vestiges of a maximum in log *K* above 423 K for $[CuCl_3]^-$. This effect, along with the rapidly increasing formation constant of $[CuCl_2]^0$, suggest that the uncharged $[CuCl_2]^0$ is probably the dominant species at high-temperatures and at low to intermediate concentrations. HKF predictions compare quite favourably with the reported data, although the model parameters for complexes were obtained only from older experimental results at 298 K, using various empirical inter-correlations among these values and the HKF equation parameters. In case of $[CuCl]^+$ the predictions are semi-quantitative, for the higher complexes the agreement is qualitative.

One of the conclusions we have drawn from these preliminary modeling attempts is that more reliable interpretation of the data requires additional measurements, namely we plan to obtain several complete new sets of data at temperatures to ~473 K for confirmation of high-temperature trends in formation constants. Another conclusion is that we need to explore alternative activity coefficient models for more authoritative assessment of thermodynamic properties in concentrated brines. Our goal is to use the experimental results to develop a model compatible with the OLI Engine (i.e. the mixed solvent electrolyte model) and Aspen Plus modeling software. The OLI mixed solvent electrolyte model (OLI Systems Inc.) is a very sophisticated computer code that provides a rigorous computation of thermodynamic properties including Gibbs free energy, enthalpy, entropy, heat capacity, etc. and is able to analyze multicomponent aqueous solutions in equilibrium with several solid phases and a vapour phase in the full range of concentrations from dilute solutions to the fused salt limit. Finally we consider the application of Mean Spherical Approximation to the modeling of activity coefficients, which could provide more theoretically justified estimates namely for polyvalent and neutral species.

4. Conclusions

UV-Vis absorption spectra were measured in acidic copper-chloride solutions at 373 K and 423 K, 9 MPa, using a constant low concentration of Cu and Cl_{tot} concentration up to 15 mol kg^{-1}. Thermodynamic formation constants of the copper-chloride complexes were retrieved from the experimental data using appropriate physical-chemical constraints. The preliminary results reported in this work are in good agreement with data and trends from the previous studies. A plan for completing the measurements and alternative modeling of activity coefficients has been developed, in order to obtain reliable thermodynamic representation of copper-chloride complexation to at least 473 K suitable for parameterizing engineering models for the copper-chloride thermochemical hydrogen production cycle. We consider these efforts a necessary step towards developing a model for even more complicated mixtures of copper-chloride complexes, including polynuclear ones, that resembles the systems proposed for the copper-chloride cycles evaluated for hydrogen production.

Acknowledgement

This work was supported by the International Association for the Properties of Water and Steam (IAPWS Young Scientist Fellowship for J.E.), the Research Centre ''Advanced Remedial Technologies and Processes'' at the Technical University of Liberec, Atomic Energy of Canada Ltd., the Ontario Research Foundation and the Natural Science and Engineering Council of Canada (NSERC).

REFERENCES

[1] Petri MC, Yildiz B, Klickman AE. US work on technical and economic aspects of electrolytic, thermochemical, and hybrid processes for hydrogen production at temperatures below 550 °C. Int J Nucl Hydrogen Prod Appl 2006;1:79–91.
[2] Naterer G, Suppiah S, Lewis M, Gabriel K, Dincer I, Rosen M, et al. Recent Canadian advances in nuclear-based hydrogen production and the thermochemical Cu-Cl cycle. Int J Hydrogen Energy 2009;34:2901–17.
[3] (a)Stolberg L, Boniface H, McMahon S, Suppiah S, York S. Development of the electrolysis reactions involved in the Cu-Cl thermochemical cycles. In: Proceedings of the International Conference on Hydrogen Production; May 5, 2009. pp. 167–177.(b)Zhang J, Xie Z, Zhang J, Tang Y, Song C, Navessin T, et al. High temperature PEM fuel cells. J Power Sources 2006;160:872–91.
[4] Fritz JJ, Königsberger E. Solubility data series: copper (I) halides and pseudohalides, vol. 65. Oxford University Press; 1996.
[5] Crerar DA, Barnes HL. Ore solution chemistry V. Solubilities of chalcopyrite and chalcocite assemblages in hydrothermal solution at 200 and 350 °C. Econ Geol 1976;7:772–94.
[6] Fontana A, van Muylder J, Winand R. Etude spectrophotometrique de solutions aqueses chlorurees de chlorure cuivreux a concentrations elevess. Hydrometallurgy 1983;11:297–314.
[7] Xiao Z, Gammons CH, Williams-Jones AE. Experimental study of copper (I) chloride complexing in hydrothermal solutions at 40–300 °C and saturated water vapor pressure. Geochim Cosmochim Acta 1998;62:2949–64.
[8] Liu W, McPhail DC, Brugger J. An experimental study of copper (I)-chloride and copper (I)-acetate complexing in hydrothermal solutions between 50 °C and 250 °C and vapor-saturated pressure. Geochim Cosmochim Acta 2001;65:2937–48.
[9] Liu W, Brugger J, McPhail DC, Spiccia L. A spectrophotometric study of aqueous copper (I)-chloride complexes in LiCl solutions between 100 °C and 250 °C. Geochim Cosmochim Acta 2002;66:3615–33.
[10] Liu W, McPhail DC. Thermodynamic properties of copper chloride complexes and copper transport in magmatic-hydrothermal solutions. Chem Geol 2005;221:21–39.
[11] Brugger J, McPhail DC, Black J, Spicca L. Complexation of metal ions in brines: application of electronic spectroscopy in the study of the Cu(II)-LiCl-H_2O system between 25 and 90 °C. Geochim Cosmochim Acta 2001;65:2691–708.

[12] Berger JM, Winand R. Solubilities, densities, and electrical conductivities of aqueous copper(I) and copper(II) chlorides in solutions containing other chlorides such as iron, zinc, sodium, and hydrogen chlorides. Hydrometallurgy 1984;12: 1261–81.
[13] Hyvärinen O, Hämäläinen M. HydroCopper™ - a new technology producing copper directly from concentrate. Hydrometallurgy 2005;77(1–2):61.
[14] Lundström M, Aromaa J, Forsen O, Hyvarinen O, Barker MH. Leaching of chalcopyrite in cupric chloride solution. Hydrometallurgy 2005;77(1–2):89.
[15] Kekesi T, Isshiki M. Electrodeposition of copper from pure cupric chloride hydrochloric acid solutions. J Appl Electrochem 1997;27:982–90.
[16] Trevani LN, Roberts JC, Tremaine PR. Copper(II)-ammonia complexation equilibria in aqueous solutions from 30 to 250 °C by visible spectroscopy. J Solution Chem 2001;30:585–622.
[17] Malinowski ER. Factor analysis in chemistry. 3rd ed. Wiley; 2002.
[18] Skoog DA, West DM. Fundamentals of analytical chemistry. Philadelphia: Saunders College Publishing; 1982.
[19] Mendham J, Denney RC, Barnes JD, Thomas MJK. Vogel's quantitative chemical analysis. 6th ed. Publisher Longman, Prentice Hall; 1999.
[20] Méndez De Leo LP, Wood RH. Conductance study of association in aqueous $CaCl_2$, $Ca(CH_3COO)_2$, and $Ca(CH_3COO)_2.nCH_3COOH$ from 348 to 523 K at 10 MPa. J Phys Chem B 2005;109(29):14243–50.
[21] Abdulagatov IM, Azizov ND. Densities and apparent molar volumes of concentrated aqueous LiCl solutions at high temperatures and high pressures. Chem Geol 2006;230:22–41.
[22] Brugger J. BeerOz, a set of Matlab routines for quantitative interpretation of spectrophotometric measurements of metal speciation in solution. Comput Geosci 2007;33:248–61.
[23] Tanger JC, Helgeson HC. Calculation of the thermodynamic and transport properties of aqueous species at high pressures and temperatures: revised equations of state for the standard partial molal properties of ions and electrolytes. Am J Sci 1988;288:19–98.
[24] Shock EL, Sassani DC, Willis M, Sverjensky DA. Inorganic species in geologic fluids: correlations among standard molal thermodynamic properties of aqueous ions and hydroxide complexes. Geochim Cosmochim Acta 1997;61:907–50.
[25] Shock EL, Helgeson HC. Calculation of the thermodynamic and transport properties of aqueous species at high pressures and temperatures; correlation algorithms for ionic species and equation of state predictions to 5 kb and 1000 °C. Geochim Cosmochim Acta 1988;52:2009–36.
[26] Sverjensky DA, Shock EL, Helgeson HC. Prediction of the thermodynamic properties of aqueous metal complexes to 1000 °C and 5 kbar. Geochim Cosmochim Acta 1997;61: 1359–421.
[27] Sverjensky DA, Hemley JJ, D'Angelo WM. Thermodynamic assessment of hydrothermal alkali feldspar-mica-aluminosilicate equilibria. Geochim Cosmochim Acta 1991; 55:989–1004.
[28] Pokrovskii VA. Calculation of the standard partial molal thermodynamic properties and dissociation constants of aqueous HCl^0 and HBr^0 at temperatures to 1000 °C and pressures to 5 kbar. Geochim Cosmochim Acta 1999;63: 1107–15.
[29] Ruaya JR, Seward TM. The ion-pair constant and other thermodynamic properties of HCl up to 350 °C. Geochim Cosmochim Acta 1987;51:121–30.
[30] Robinson RA. The dissociation constant of hydrochloric acid. Trans Faraday Soc 1936;32:734–44.
[31] Marsh ARW, McElroy WJ. The dissociation constant and Henry's law constant of HCl in aqueous solutions. Atmos Environ 1985;19:1075–80.
[32] Pitzer KS. Activity coefficients in electrolyte solutions. 2nd ed. CRC Press; 2000.
[33] Holmes HF, Mesmer RE. Thermodynamic properties of aqueous solutions of the alkali metal chlorides to 250 °C. J Phys Chem 1983;87:1242–55.
[34] Pokrovskii VA, Helgeson HC. Calculation of the standard partial molal thermodynamic properties of KCl^0 and activity coefficients of aqueous KCl at temperatures and pressures to 1000 °C and 5 kbar. Geochim Cosmochim Acta 1997;61:2175–83.